Physical understanding of the bending of nanostructures caused by cellular force

Hang Zang and Xinlei Li ⬤ [*]

MOE Key Laboratory of Laser Life Science and Guangdong Provincial Key Laboratory of Laser Life Science,
College of Biophotonics, South China Normal University, Guangzhou 510631, China

The bending of nanostructures (NSs), such as nanopillars and nanowires, caused by cell adhesion is an interesting phenomenon and is important for the measurements of cellular forces, understanding the biological behavior of cells, and disease diagnosis. However, which factors are related to the bending of NSs and how the factors affect bending displacement are still not well understood. Here, we establish an analytic thermodynamic theory to study the bending mechanism of NSs caused by cellular force during the cell adhesion process, and analyze the factors affecting bending displacement. It is found that the bending of NSs is determined by the competition between the stretching energy of the membrane and the strain energy of the NSs. The bending displacement can be evaluated based on our model.

I. INTRODUCTION

Artificial nanostructures (NSs) have become key materials for cellular activity regulation, intracellular delivery and detection, specific cell captures, etc., due to the controlled interactions between NSs and biological cells [1–5]. Recently, high-aspect-ratio vertical NSs arrays, such as nanowires and nanopillars, have been widely applied as a new biological tool to investigate cell adhesion [6–10], migration [4,5], and capture [11–14]. Interestingly, over the course of the study, the researchers found that nanowires and nanopillars with small radius would bend due to cell growth on their surfaces [15–19].The bending of NSs provides a method to detect cellular forces by calculating from the displacement of NSs. The method not only provides a good basis for live-cell force measurements, but also is potentially useful for oncology, disease diagnosis, and drug development [15,16]. The developments of the above applications are all related to the interactions between NSs and cells. However, there are only a few theoretical analyses to elucidate the mechanisms of cell-NSs interactions. Moreover, the several existing theoretical models all consider NSs to be rigid and cannot be applied to the bending of NSs [20–22]. So far it is still not well understood how the influence factors affect cell-NSs interactions, especially the bending of NSs. To the best of our knowledge, the bending of NSs is used to detect cellular forces only according to the displacement of NSs in experiments, but how to choose appropriate NSs corresponding to a detectable displacement is still unclear, which requires us to know what factors are related to the bending of NSs and how the factors affect displacement of NSs.

In this work, we propose an analytic thermodynamic approach to quantitatively study the bending mechanism of NSs caused by cellular force during cell adhesion,

and analyze the factors affecting bending displacement. We find that the bending of NSs can effectively release the stretching energy of the membrane but cause the increase of strain energy of NSs, and the bending displacement of NSs is determined by the balance between the stretching energy of the membrane and the strain energy of the NSs.

II. THEORETICAL MODEL

When a cell adheres to the surface with an array of vertical NSs, such as nanowires and nanopillars, the release of adhesion energy can drive the contact membrane to extend into the space between the NSs. If the vertical NSs are regarded as rigid, considering the contributions of contact adhesion energy, bending energy, and stretching energy of the deformed membrane, the equilibrium state of cell adhesion, i.e., adhesion degree, can be analyzed by minimizing the free energy change where [21,23]

$$\Delta E = -\int_{S_{ad}} \gamma \, dA + \int_{S_{bend}} \left[\frac{\kappa}{2}(c_1 + c_2 - c_0)^2 \right] dA + \frac{1}{2}\lambda \frac{\Delta S^2}{S_0},$$

(1)

where γ is the adhesion energy per unit area between the cell membrane and the surface; S_{ad} denotes the adhesion area between the cell and the surface; κ is the bending modulus of the membrane; c_1 and c_2 are two principal curvatures of the bending membrane surface; S_{bend} is the area of bending in the membrane; λ is the stretching modulus of the membrane; ΔS and S_0 are, respectively, the area change and initial total area of the membrane; and $\Delta S = S - S_0$, with S indicating the total area of the membrane during the adhesion process. The first term is the chemical energy released by the adhesion, the second term represents the total bending energy of the cell membrane calculated by the Helfrich model [24], and the third term is the stretching energy penalty [25].
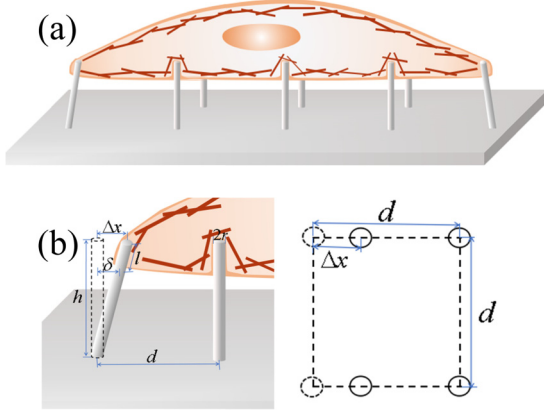
────────
[*]xlli@scnu.edu.cn

FIG. 1. (a) Schematic illustration of the cell adhesion on the surface of the nanopillar array. (b) The enlarged views of the bending of nanopillar caused by cell adhesion.

However, the thin and long NSs are easy to bend or distort because of the drag of the stretching cell membrane. In this case, the vertical NSs cannot be regarded as rigid. The distortion of NSs can partially release the stretching energy of the membrane, but the strain energy stored in distorted NSs increases. Therefore, we should consider the effects of strain energy stored in NSs and the change of stretching energy caused by the NSs bending.

The bending of NSs most often occurs at the edge of the contact area because the outermost NSs suffer from an unbalanced pulling force toward the interior of the contact interface [15]. Therefore we select a period square domain at the edge of the contact area as a study object to analyze the free energy change caused by cell adhesion and the NSs bending, as shown in Fig. 1, in which nanowires or nanopillars with a radius of r, height of h, and center-to-center spacing of d are considered to be located at the sites of an ideal square lattice. When the bending of NSs occurs, the area of the membrane in the period square domain can be approximatively expressed as $S = d(d - \delta) + 2n\pi rl$, where l is the adhesion depth, n represents the valid number of NSs adhered by the cell membrane, and δ is the displacement of the nanowire at the bottom of the cell where $\delta = (h - l)\Delta x/h$ (Δx is the displacement of the NS tip, as shown in Fig. 1). It should be noted that the adhesion depth, l, is assumed to be identical for all NSs in the square domain. The identical value of adhesion depth for all NSs corresponds to the minimal area of the membrane in the space among the NSs, which means the smallest stretching of the membrane and the lowest stretching energy. The assumption has been used in some theoretical studies on cell settling on NS arrays without the bending of NSs [20,21]. In fact, adhesion depth may vary from one NS to another when bending occurs, which depends on the bending degree and the shape of the entire cell. Because the displacement of the NSs is much smaller than the height of the NSs, we neglect the variation of adhesion depth in order to simplify the model. Therefore the stretching energy in Eq. (1) can be calculated by

$$\frac{1}{2}\lambda \frac{\Delta S^2}{S_0} = \frac{\lambda[2n\pi rl - d(h - l)\Delta x/h]^2}{2d^2}. \tag{2}$$

In calculating the strain energy of bending NSs, we applied the Cartesian first theorem. According to the Cartesian first theorem, we can know that the partial derivative of strain energy to a real displacement is numerically equal to the corresponding external force applied at this true displacement. It can be expressed as

$$P = \partial U / \partial \delta, \tag{3}$$

where P is the stress and U is the strain energy. The relationship between deflection and stress is satisfied [26]

$$P = \frac{3YI}{L^3}\delta, \tag{4}$$

where Y is the Young's modulus of the NSs, I is the inertia of the NSs and $I = \pi r^4/64$, and $L = h - l$. After we convert the parameter δ to the top offset Δx [$\delta = (h - l)\Delta x/h$], according to Eqs. (3) and (4), we can obtain the relationship between the strain energy of a single NS and the tip offset where

$$E_{\mathrm{NS}} = \frac{3YI\Delta x^2}{2h^2(h - l)}. \tag{5}$$

In a period square domain, the number of bending NSs is 1 (two half NSs), and the valid number of NSs adhered by the cell membrane, n, is considered to be 3/2 (two half NSs and two quarter NSs). After adding up the adhesion energy ($-2n\pi\gamma rl$), the bending energy of the cell membrane ($n\pi\kappa l/r$) [21], the stretching energy [Eq. (2)], and the strain energy of the NSs [Eq. (5)], we can obtain the total free energy change as

$$\Delta E_{\mathrm{total}} = -3\pi\gamma rl + \frac{3\pi\kappa l}{2r} + \frac{\lambda[3\pi rl - d(h - l)\Delta x/h]^2}{2d^2}$$
$$+ \frac{3Y\pi r^4\Delta x^2}{128h^2(h - l)}. \tag{6}$$

The total free energy change is the functions of the displacement of NSs (Δx) and the adhesion depth of the cell (l). Therefore, we can find the equilibrium stage of the cell adhesion by minimizing the total free energy change. From $\partial\Delta E_{\mathrm{total}}/\partial\Delta x = 0$, $\Delta E_{\mathrm{total}}$ will be minimal under a fixed l when

$$\Delta x = \frac{192\pi\lambda rhl(h - l)^2}{d[64\lambda(h - l)^3 + 3\pi Yr^4]}. \tag{7}$$

We can determine the equilibrium stage of the cell adhesion accompanied by NSs bending through calculating the minimum of $\Delta E_{\mathrm{total}}$ in Eq. (6) and obtain the relation of displacement of NSs and adhesion depth according to Eq. (7).

III. RESULTS AND DISCUSSION

In order to better compare with experimental observations, we take cell adhesion on the typical Si nanopillars array as an example in our model [15,17,19]. Firstly, we select the parameters of Si nanopillars surface topography as $r = 100$ nm, $h = 10 \mu$m, and $d = 2 \mu$m according to experimental data [17] to study the physical mechanism of NSs bending. The other parameters in our calculations are as follows: $Y = 18.5 \times 10^{11}$ dyn/cm^2 [27], $\gamma = 0.25 \, k_{\mathrm{B}}T/$nm^2 [28], $\kappa = 20 \, k_{\mathrm{B}}T/$nm^2 [29,30], and $\lambda = 5 \, k_{\mathrm{B}}T/$nm^2 [29]. In
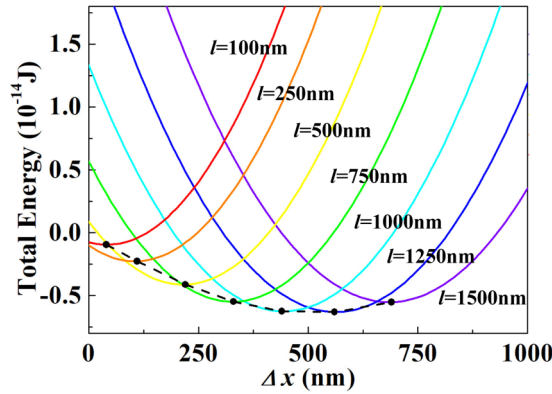
FIG. 2. The calculated ΔE_{total} as the function of Δx under different values of l from 100 to 1500 nm based on Eq. (6).

order to investigate the evolution of cell adhesion and NSs bending, we calculated the ΔE_{total} as the function of Δx under the different value of l from 100 to 1500 nm based on Eq. (6), as shown in Fig. 2. We find that ΔE_{total} first decreases and then increases with the increase of Δx, and has a minimum value which corresponds to the stable state of the NSs bending under a fixed value of l. The appearance of the minimum of ΔE_{total} is caused by the competition between the stretching energy of the membrane and the strain energy of the NSs. The bending of nanopillars results in the decrease of stretching energy [Eq. (2)] but an increase of strain energy of NSs [Eq. (5)] by the decrease of Δx or δ. For the low bending degree (small Δx), the decrease of stretching energy is approximately in a direct ratio to Δx, and the increase of strain energy of the NSs is proportional to the second order of Δx. Therefore, in this case, the decrease of the stretching energy plays a more important role than the increase of strain energy, so ΔE_{total} will decrease with increasing Δx. However, for large Δx, E_{NS} becomes greater and increases rapidly due to the increase of Δx, which eventually leads to the increase of ΔE_{total} with increasing Δx. Further comparing of the values of minimum of ΔE_{total} under different l, we can also find that the minimum of ΔE_{total} for different l first decreases and then increases with increasing l (as shown by the dashed curve in the Fig. 2). This suggests that the adhesion of cells on NSs is not deeper and more stable. In other words, cells cannot always release the total free energy by adhering downward. The minimum of the dashed curve corresponds to the most stable state of the adhesion system in which Δx is about 500 nm and l is between 1000 and 1250 nm.

In order to more directly determine the most stable state, we calculated the values of ΔE_{total} as the functions of l and Δx from Eq. (6), as shown in Fig. 3(a). The line in the figure represents the calculated values of Δx as the function of l from Eq. (7) which tallies well with the minimum of numerical distribution of ΔE_{total} according to Eq. (6). To distinguish the evolution direction of adhesion, we mark the line as a solid line before the minimum of ΔE_{total}, and a dashed line after the minimum of ΔE_{total}. The dividing point between the solid line and the dashed line represents the minimum of ΔE_{total}, which corresponds to the most stable state, so we can obtain the most stable state through analyzing the value distribution of ΔE_{total} from Eq. (6). In addition to this method, we can
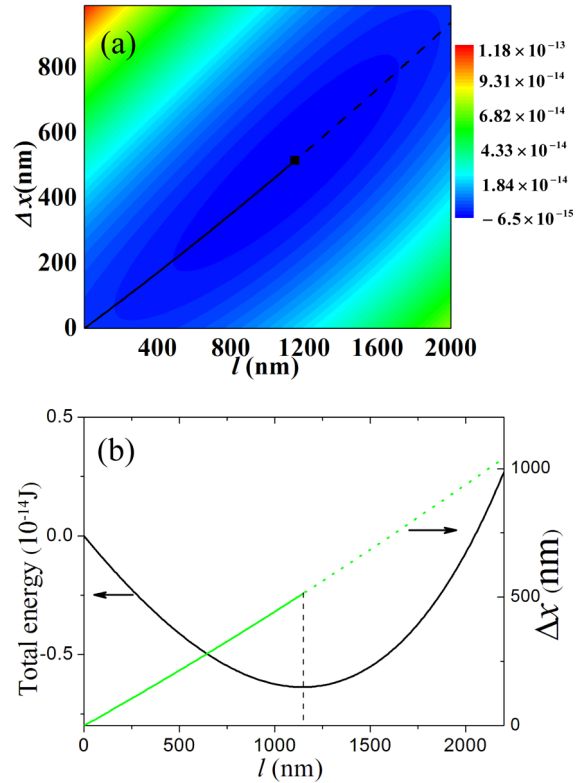

FIG. 3. (a) The calculated ΔE_{total} as the functions of l and Δx from Eq. (6). The black line represents the calculated values of Δx as the function of l from Eq. (7). (b) The calculated ΔE_{total} and Δx as the function of l using Eqs. (6) and (7). The line of Δx is divided into a solid part and a dashed part according to the minimum of ΔE_{total}.

first calculate the relation of Δx and l from Eq. (7), and then bring Δx of Eq. (7) into Eq. (6) to calculate the values of ΔE_{total}, and finally find the dividing point (i.e., the most stable state) according to the variation trend of ΔE_{total}. Figure 3(b) shows the calculated results based on the method. The line of Δx is divided into a solid part and a dashed part according to the minimum of ΔE_{total}. The dividing point in Fig. 3(b) is consistent with that in Fig. 2(a). Both of them show that there is a minimum of ΔE_{total} when $l \approx 1150\,\text{nm}$ and $\Delta x \approx 510\,\text{nm}$. The theoretical results agree with experimental observations in which Si nanopillars with the same parameters of surface topography as that in our calculations have clearly been curved by cell adhesion [17].

The experimental observations have shown that the bending of NSs strongly depends on the surface geometry of NSs such as their radius, height, and center spacing. In this connection, we can investigate the effects of the geometry of nanopatterned surfaces on the bending of NSs using our proposed model. Figure 4(a) illustrates the effects of the radius of nanopillars on the bending degree. The figure shows the displacement of the NS tip Δx as the function of adhesion depth l under different radius when $h = 10\,\mu\text{m}$ and $d = 2\,\mu\text{m}$. The most stable states of the adhesion process are marked by the dividing points between the solid line and the dashed line in which we adopt the same method as that in Fig. 3(b). Obviously, the thin nanopillars have large displacement and adhesion depth, which means that thin
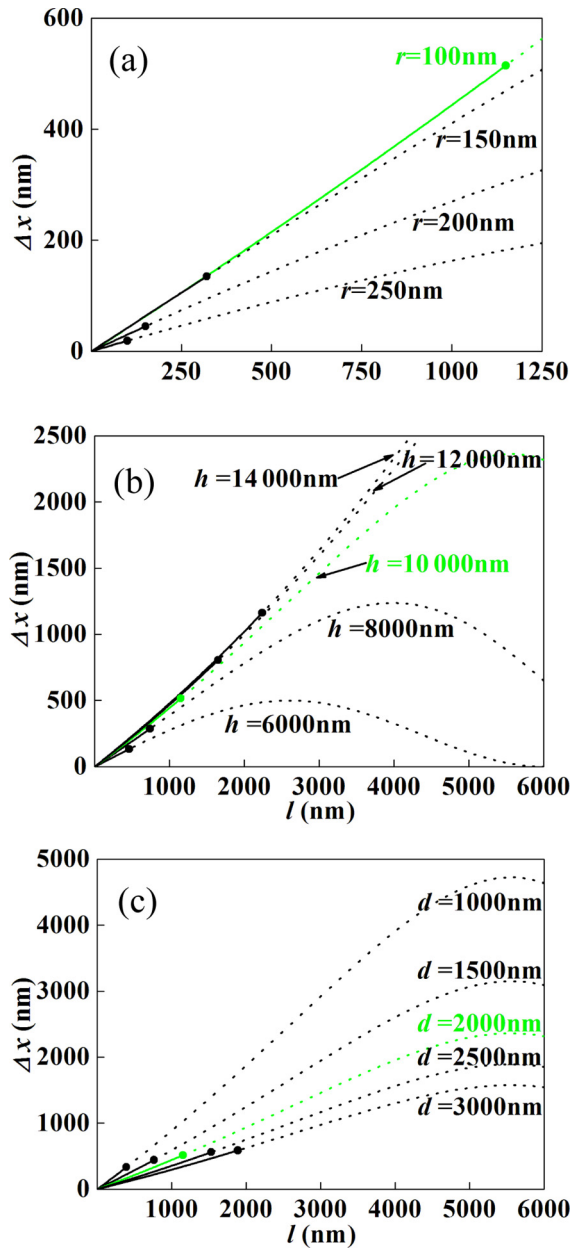
FIG. 4. Effects on the predicted bending displacement Δx under different (a) radius, (b) height, and (c) spacing. The green (light gray) lines are the tendencies for cell adhesion to NSs of dimensions $r = 100$ nm, $h = 10\,\mu$m, and $d = 2\,\mu$m (as used in Figs. 2 and 3), while the other lines give the tendencies when the (a) NS radius, (b) NS height, or (c) spacing are independently varied (with r fixed to 100 nm, h fixed to $10\,\mu$m, or d fixed to $2\,\mu$m, respectively).

nanopillars can be adhered deeper by the cell and areeasier to bend than thick nanopillars. The effects of the nanopillars' height on the bending degree are shown by Fig. 4(b) which suggests that the long nanopillars have larger displacement than short nanopillars. The reasons for the easier bend of thin and long nanopillars are that a large bending degree can effectively reduce the stretching energy of the membrane [Eq. (2)], and the bending of thin and long nanopillars results in a relatively lower strain energy than that of thick and short nanopillars under the same tip offset [Eq. (5)]. These

modeling results show good agreement with the experimental results in which high-aspect-ratio (thin and long) nanopillars undergo larger deflections than low-aspect-ratio (thick and short) nanopillars under cellular forces during the adhesion process [15–17].

Figure 4(c) shows the effects of the center-to-center spacing (i.e., density) of nanopillars on the bending degree. The results suggest that the most stable states of adhesion on the nanopillars with small spacing (high density) correspond to small displacement and small adhesion depth. Small adhesion depth is because the membrane suffers from intensive stretching and bending during the adhesion on the sidewalls as a result of the small space among the nanopillars [21]. Meanwhile, it only takes a small displacement of nanopillars to effectively release the stretching energy because the initial area of the membrane (d^2) is small in the case with small spacing. The modeling results also agree well with experimental observations that high-density nanopillars have no visible bending and the cells are characteristically adherent to the tips of the nanopillars (small adhesion depth) [17–19], but low-density nanopillars show obvious bending and large adhesion depth [18,19].

It should be noted that we consider that the material properties of the cell membrane are uniform and homogeneous in our model. In fact, cell membranes are heterogeneous and typically comprise nanoscale lipid clusters. The nanoscale clusters in cell membranes can serve as platforms to recruit membrane proteins for various biological functions. Recently, Li *et al.* studied how these nanoclusters respond to physical contacts between cells and explored how the adhesion of cell membranes affects the stability and coalescence of clusters enriched in receptor proteins using a statistical mechanics model and Monte Carlo simulations [31]. Their results show that intercellular receptor-ligand binding and membrane shape fluctuations can lead to receptor aggregation within the adhering membranes. In our model, because it is difficult to describe intuitively and quantitatively the contribution of the nanoscale clusters in cell membrane, we ignore the effects of heterogeneity of the cell membrane. Besides, we also neglect the effect of cytoskeleton deformation in our model. Wang and Li reported that deformation of the cytoskeleton can influence the engulfing process of the cylindrical nanoparticles [32]. Here we assume that the resistance of cell adhesion is dominated by membrane deformation, so we only consider the deformation energy of the membrane in Eq. (1).

Beyond that, we describe the ability of cell adhesion on the NSs surface by the adhesion energy per unit area, γ, which is considered as a constant during the adhesion process. In reality, adhesion of biological membranes is a highly cooperative process. Krobath *et al.* predicted theoretically that shape fluctuations of the elastic membranes lead to cooperative binding of receptors and ligands [33]. Recently, Steinkühler *et al.* provided some of the first experimental evidence of cooperative binding due to suppression of membrane fluctuations based on fluorescence experiments [34]. These results suggest that the ability of cell adhesion ought to be varying with membrane fluctuations. Because the surface of the NSs has a high specific surface area and high surface roughness, it is difficult to express quantitatively the effects of membrane fluctuations on the ability of cell adhesion, so we consider that

adhesion energy per unit area, γ, remains constant in order to simplify our model.

IV. CONCLUSIONS

In conclusion, we present an analytic model to study the bending of NSs caused by cellular force during the cell adhesion process and provide a simple method to anticipate the bending degree of NSs. We find that the bending of NSs is determined by the balance of the competition between the stretching energy of the membrane and the strain energy of NSs. The bending of NSs can release the stretching energy of the membrane but cause the increase of strain energy of the NSs. Modeling results suggests that thin, long, and sparse nanopillars or nanowires are easy to bend. Agreement between theoretical results and experimental observations implies that the established model could be applicable to understanding the basic physical mechanism of the bending of NSs during the cell adhesion process and help us choose appropriate NSs corresponding to a detectable displacement.

[1] L. A. Dykman and N. G. Khlebtsov, Chem. Rev. **114**, 1258 (2014).

[2] P. Sharma, H. A. Cho, J. W. Lee, W. S. Ham, B. C. Park, N. H. Cho, and Y. K. Kim, Nanoscale **9**, 15371 (2017).

[3] H. J. Yoon, T. H. Kim, Z. Zhang, E. Azizi, T. M. Pham, C. Paoletti, J. Lin, N. Ramnath, M. S. Wicha, D. F. Hayes, D. M. Simeone, and S. Nagrath, Nat. Nanotechnol. **8**, 735 (2013).

[4] H. Jeon, S. Koo, W. M. Reese, P. Loskill, C. P. Grigoropoulos, and K. E. Healy, Nat. Mater. **14**, 918 (2015).

[5] J. Park, D. H. Kim, H. N. Kim, C. J. Wang, M. K. Kwak, E. Hur, K. Y. Suh, S. S. An, and A. Levchenko, Nat. Mater. **15**, 792 (2016).

[6] A. S. G. Curtis, N. Gadegaard, M. J. Dalby, M. O. Riehle, C. D. W. Wilkinson, and G. Aitchison, IEEE Trans. Nanobiosci. **3**, 61 (2004).

[7] J. Park, S. Bauer, K. A. Schlegel, F. W. Neukam, K. von der Mark, and P. Schmuki, Small **5**, 666 (2009).

[8] N. W. Karuri, T. J. Porri, R. M. Albrecht, C. J. Murphy, and P. F. Nealey, IEEE Trans. Nanobiosci. **5**, 273 (2006).

[9] I. Melnichuk, A. Choukourov, M. Bilek, A. Weiss, M. Vandrovcová, L. Bačáková, J. Hanuš, J. Kousal, A. Shelemin, P. Solař, D. Slavínská, and H. Biederman, Appl. Surf. Sci. **351**, 537 (2015).

[10] R. Capozza, V. Caprettini, C. A. Gonano, A. Bosca, F. Moia, F. Santoro, and F. De Angelis, ACS Appl. Mater. Interfaces **10**, 29107 (2018).

[11] S. Wang, Y. Wan, and Y. Liu, Nanoscale **6**, 12482 (2014).

[12] S. K. Lee, G. S. Kim, Y. Wu, D. J. Kim, Y. Lu, M. Kwak, L. Han, J. H. Hyung, J. K. Seol, C. Sander, A. Gonzalez, J. Li, and R. Fan, Nano Lett. **12**, 2697 (2012).

[13] S. Bonde, N. Buch-Manson, K. R. Rostgaard, T. K. Andersen, T. Berthing, and K. L. Martinez, Nanotechnol. **25**, 362001 (2014).

[14] H. Cui, B. Wang, W. Wang, Y. Hao, C. Liu, K. Song, S. Zhang, and S. Wang, ACS Appl. Mater. Interfaces **10**, 19545 (2018).

[15] Z. Li, J. Song, G. Mantini, M.-Y. Lu, H. Fang, C. Falconi, L.-J. Chen, and Z. L. Wang, Nano Lett. **9**, 3575 (2009).

[16] W. Hällström, M. Lexholm, D. B. Suyatin, G. Hammarin, D. Hessman, L. Samuelson, L. Montelius, M. Kanje, and C. N. Prinz, Nano Lett. **10**, 782 (2010).

[17] M. A. Bucaro, Y. Vasquez, B. D. Hatton, and J. Aizenberg, ACS Nano **6**, 6222 (2012).

[18] N. Buch-Månson, A. Spangenberg, L. P. C. Gomez, J.-P. Malval, O. Soppera, and K. L. Martinez, Sci. Rep. **7**, 9247 (2017).

[19] N. Buch-Månson, D.-H. Kang, D. Kim, K. E. Lee, M.-H. Yoon, and K. L. Martinez, Nanoscale **9**, 5517 (2017).

[20] N. Buch-Månson, S. Bonde, J. Bolinsson, T. Berthing, J. Nygård, and K. L. Martinez, Adv. Funct. Mater. **25**, 3246 (2015).

[21] J. Zhou, X. Zhang, J. Sun, Z. Dang, J. Li, X. Li, and T. Chen, Phys. Chem. Chem. Phys. **20**, 22946 (2018).

[22] X. Xie, A. M. Xu, M. R. Angle, N. Tayebi, P. Verma, and N. A. Melosh, Nano Lett. **13**, 6002 (2013).

[23] J. Zhou, Y. Xiong, Z. Dang, J. Li, X. Li, Y. Yang, and T. Chen, J. Mater. Sci. **54**, 4236 (2019).

[24] W. Helfrich, Z. Naturforsch., C: Biochem., Biophys., Biol., Virol. **28**, 693 (1973).

[25] X. L. Li and T. S. Chen, Phys. Rev. E **93**, 052419 (2016).

[26] E. M. Lifshitz, A. M. Kosevich, and L. P. Pitaevskii, in *Theory of Elasticity*, 3rd ed. (Butterworth-Heinemann, Oxford, 1986).

[27] X. L. Li, C. X. Wang, and G. W. Yang, Prog. Mater. Sci. **64**, 121 (2014).

[28] X. L. Li and D. Xing, Appl. Phys. Lett. **97**, 153704 (2010).

[29] S. Mirigian and M. Muthukumar, J. Chem. Phys. **139**, 044908 (2013).

[30] Y. Sun, T. L. Sun, and H. W. Huang, Biophys. J. **107**, 2082 (2014).

[31] L. Li, J. Hu, B. Różycki, and F. Song, Nano Lett. **20**, 722 (2020).

[32] J. Wang and L. Li, J. R. Soc., Interface **12**, 20141023 (2015).

[33] H. Krobath, B. Różycki, R. Lipowsky, and T. R. Weikl, Soft Matter **5**, 3354 (2009).

[34] J. Steinkühler, B. Różycki, C. Alvey, R. Lipowsky, T. R. Weikl, R. Dimova, and D. E. Discher, J. Cell Sci. **132**, jcs216770 (2019).